Carrier density and magnetism in graphene zigzag nanoribbons

J. Jung* and A. H. MacDonald
Department of Physics, University of Texas at Austin, Austin, Texas 78712, USA
(Received 15 April 2009; revised manuscript received 3 June 2009; published 25 June 2009)

The influence of carrier density on magnetism in a zigzag graphene nanoribbon is studied in a π-orbital Hubbard-model mean-field approximation. Departures from half filling alter the magnetism, leading to states with charge-density variation across the ribbon and parallel spin alignment on opposite edges. Finite carrier densities cause the spin density near the edges to decrease steadily, leading eventually to the absence of magnetism. At low doping densities the system shows a tendency to multiferroic order in which edge charges and spins are simultaneously polarized.

DOI: 10.1103/PhysRevB.79.235433 PACS number(s): 75.75.+a, 73.20.−r, 73.22.−f, 77.80.−e

I. INTRODUCTION

Graphene sheets and related carbon-based nanomaterials have attracted attention recently after seminal experiments[1,2] revealed novel physics related to their unique electronic structure.[3] In graphene nanoribbons[4–24] lateral confinement leads to size quantization and to one-dimensional (1D) conduction channels whose properties depend qualitatively on edge termination character. Neutral zigzag-terminated ribbons have attracted particular attention because they have a flatband, perfectly flat in simple π-band models, pinned to the Fermi level. In self-consistent field (SCF) theories, including *ab initio* spin-density-functional theories (DFTs), the flatband leads to robust magnetic order. Ferromagnetic (F) alignment of spins at the zigzag edges is predicted also in treatments going beyond mean field.[7,8] Although the reliability of SCF theories is uncertain and not yet tested experimentally, interest in zigzag-edge magnetism has remained strong because of potential for interesting applications in nanoelectronics.[18]

Most studies of the electronic structure of zigzag-terminated graphene ribbons have focused on properties of the neutral system or systems with substitutional doping.[25] We study the role of gate voltage induced changes in carrier density, i.e., gate doping. A related work in the low-carrier doping regime with an additional neutralizing background charge explored the possibility of stable noncollinear (NC) magnetic states.[26] In neutral systems, SCF theories predict edge magnetization in graphene nanoribbons with opposite spin polarizations on opposite edges.[4,9,15] In theoretical studies of locally gated zigzag-ribbon junctions usually the noninteracting electronic structure is assumed,[27–33] neglecting the possibility of doping-dependent interaction-driven rearrangements. In this work we show that gate doping leads to changes in charge distribution, spin configuration, and total net spin polarization, which are accompanied by important modifications in electronic structure.

Our study is based on the π-orbital Hubbard-model SCF theory for the magnetic properties of graphene nanostructures,[17,34–36] in which an electron of spin σ in site i experiences a repulsive interaction proportional to the density of opposite-spin electrons $n_{i\bar{\sigma}}$. The Hubbard-model SCF theory is broadly consistent with DFT calculations when the interaction parameter U is chosen appropriately. The π-orbital Hartree-Fock theory reduces to the Hubbard model when only the on-site Coulomb interactions are retained. We have chosen to use a Hubbard interaction parameter $U=2$ eV which reproduces in the undoped case the band gaps obtained by microscopic density-functional theory in the local-density approximation (LDA). This value is smaller than other estimates[34] but has been adopted with a similar motivation in some other recent work.[17]

The Hubbard-model mean-field Hamiltonian for each spin σ is

$$H_\sigma = -\gamma_0 \sum_{\langle i,j \rangle} c_{i\sigma}^\dagger c_{j\sigma} + U \sum_i n_{i\bar{\sigma}} n_{i\sigma} c_{i\sigma}^\dagger c_{i\sigma} + v_{\text{ext}} \sum_i c_{i\sigma}^\dagger c_{i\sigma}$$

consist of a nearest-neighbor tight-binding term with hopping $\gamma_0=2.6$ eV connecting lattice sites i and j, the Hubbard term representing electron-electron interactions, and an ex-

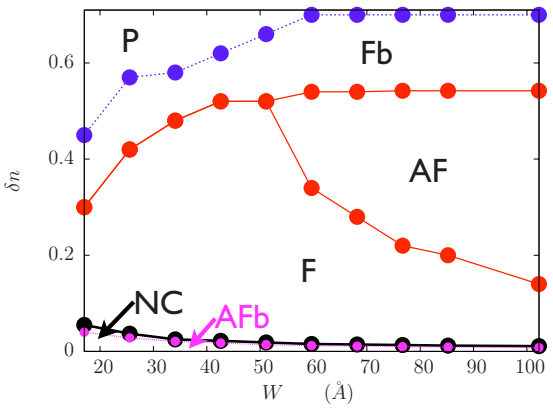

FIG. 1. (Color online) Hubbard-model SCF-theory phase diagram as a function of doping per length δn (defined in the text) and ribbon width W for nearest-neighbor hopping $\gamma_0=2.6$ eV. The on-site repulsion strength was chosen to have a value $U=2$ eV which reproduce the ribbon band gaps obtained in the LDA-DFT calculations in Ref. 17. We used 1200 k points for Brillouin-zone sampling. The energetic preference for opposite spins (AF) on opposite edges is replaced by a preference for parallel F spins at larger doping. Above a critical doping $\delta n \sim 0.7$ the SCF calculation does not find magnetic states. Solutions at finite doping sometimes (AFb and Fb) break the inversion symmetry of the ribbon. When NC is allowed canted spin solutions midway between AF and F configuration become energetically favored at low doping.

ternal potential term accounting for the interaction with the constant positive background charge proportional to a coefficient we choose to be $v_{\rm ext}=-U$. Given the uncertainty of predictions implied by particular versions of SCF theory, the advantages of this relatively simple model often outweigh disadvantages. Because the magnetism in zigzag ribbons is essentially one dimensional, we measure doping δn in units of the number of excess electrons per repeat distance $a=2.46$ Å along the edge. The corresponding areal density $\delta n_{\rm 2D}=\delta n/W$, where the ribbon width $W=\sqrt{3}Na/2$ and N is the number of atom pairs per ribbon unit cell.

II. SCF SOLUTIONS AT FINITE DOPING

The main players in zigzag-edge magnetism are the flat-band states which occupy one-third of the one-dimensional ribbon Brillouin zone (BZ) and are localized[11] near the ribbon edges, most strongly so near the BZ boundary $|k|\sim\pi/a$. In the undoped SCF ground state, electrons of opposite spin are localized near opposite edges of the ribbon and a gap[19] $\Delta\propto W^{-1}$ separates occupied valence and empty conduction-band ribbon states. By appealing to particle-hole symmetry we can limit our discussion of doping to the n-type case in which electrons start filling the conduction band. The doping causes charge-density variation across the ribbon and to a complicated competition between band and interaction energies manifested by the variety of SCF equation solutions classified below. We label solutions as AF (opposite) or F (parallel) to indicate the relative alignment of spins on opposite edges. The label NC is used indicate noncollinear spin solutions. The label b is applied for solutions which break inversion symmetry across the ribbon in a way which will be explained in more detail later. Finally we use the letter P to designate a paramagnetic state with no local spin polarization. The phase diagram in Fig. 1 illustrates the sequence of transitions AF→NC→F→Fb→P in narrower ribbons. In wider ribbons we find an additional AF state region between the F and Fb regimes.

The total energy per unit cell consist of a sum over all the occupied single-particle eigenvalues $\varepsilon_{km\sigma}$ labeled with k and m the band index divided by N_K the total number of k points minus a term to account for the double-counting correction in the interaction

$$E=\frac{1}{N_K}\sum_{km\sigma}^{\rm occ}\varepsilon_{km\sigma}-\frac{U}{2}\sum_{i\sigma}n_{i\sigma}^{\rm local}n_{i\bar{\sigma}}^{\rm local},$$

where the occupations $n_{i\sigma}^{\rm local}$ are evaluated in the local frame at lattice site i where spin is diagonal. Their differences between different self-consistent solutions are shown in Fig. 2 for a particular ($N=8$) ribbon width when only collinear spin solutions are considered. In the collinear scheme the energy associated with breaking inversion symmetry across the ribbons is always small and the main trend is a crossover from antiferromagnetic (AF) solutions at small δn to ferromagnetic solutions for $\delta n\gtrsim 0.04$ to nonmagnetic solutions for $\delta n\gtrsim 0.4$. For the F-type solutions and those with broken charge symmetry the system has a nonzero net spin polarization as a function of doping density. The doping dependence

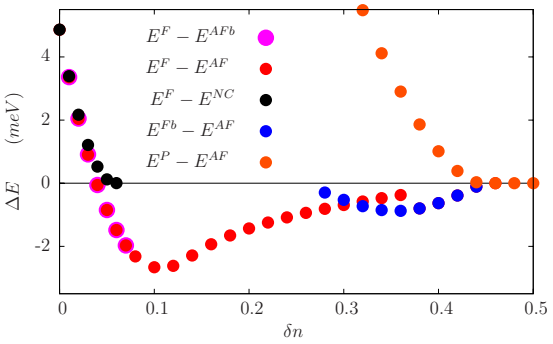

FIG. 2. (Color online) Total energy differences per edge atom between the AF (or AFb) and F, Fb, or P states as a function of doping δn for a relatively narrow ribbon with $N=8$ atom pairs per unit cell. For low doping AFb-type solutions with broken charge symmetry are energetically favored over AF solutions although the energy difference is very small. The NC spin solutions are lowest in energy in the weakly doped regime.

of spin polarization is illustrated for the same $N=8$ ribbon width in Fig. 3. Each of the solution types identified in Fig. 1 is associated with particular electronic-structure features which are illustrated in Fig. 4. For the AF solution, finite doping requires that states above the interaction-induced gap be occupied. For small doping electrons start occupying states near the conduction-band minima. [See Fig. 4.] These additional electrons suffer a large energy penalty due to the neutral solution band gap and have lower energy when spin polarized. The resulting half-metallic solution in the spin-collinear scheme implies a nonzero overall spin polarization in the system and is accompanied by a breaking of charge-distribution symmetry around the ribbon center. This asymmetric charge distribution is a combined effect of the net spin polarization and the character of the AF solution at the neutrality point, in which electrons with opposite spin polarizations are concentrated on opposite edges.[19] If both up- and down-spin bands were equally occupied there would be no charge-distribution asymmetry around the ribbon center.

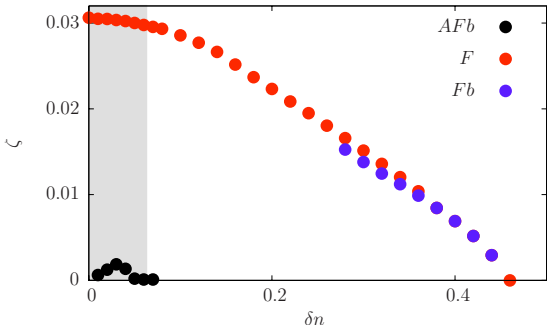

FIG. 3. (Color online) Net spin polarization obtained from the total electron spin densities $\zeta=(n_\uparrow-n_\downarrow)/(n_\uparrow+n_\downarrow)$ for AFb, F, and Fb solutions as a function of doping. AFb solutions collapse into AF solutions with zero net spin polarization for high enough doping. F and Fb configurations also progressively lose net spin polarization as they approach the nonmagnetic P limit. The shaded region represents the doping regime where noncollinear solutions are favored energetically.

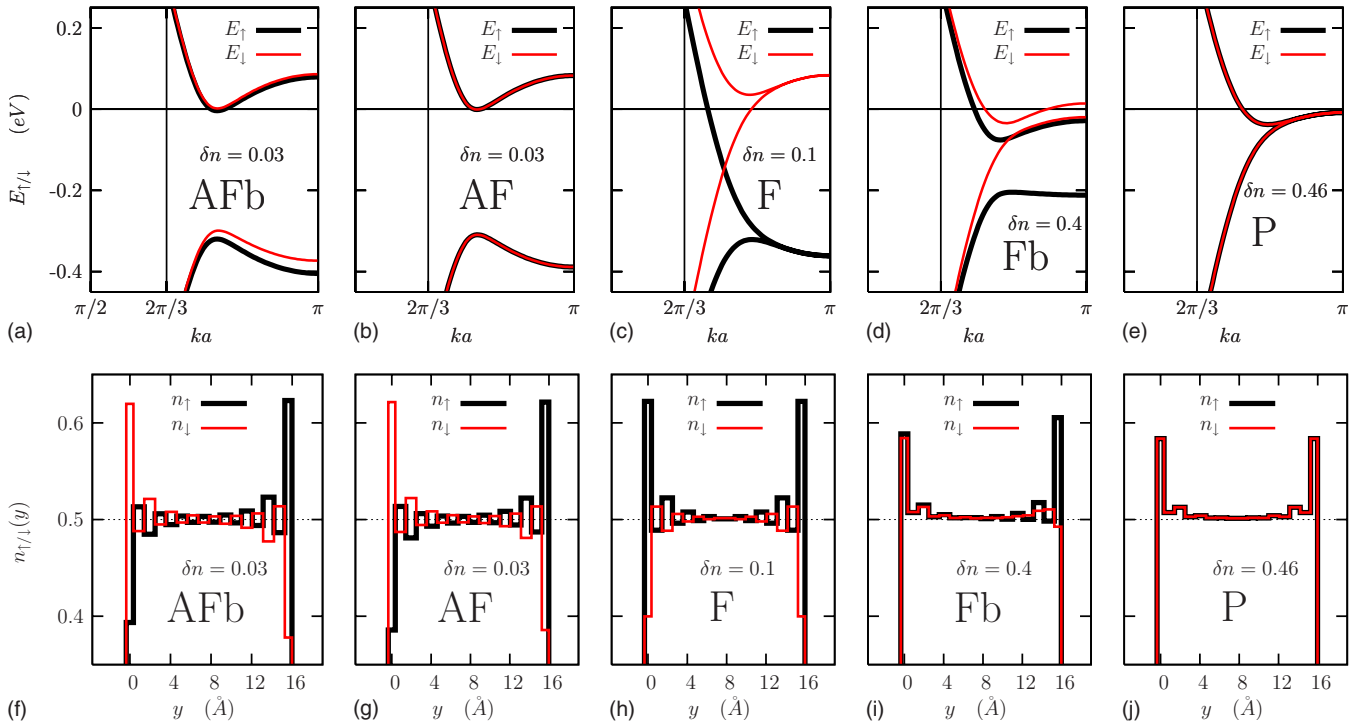

FIG. 4. (Color online) *Upper row*. Band structures corresponding to AFb, AF, F, Fb, and P spin collinear solutions of the Hubbard-model SCF equations for a zigzag nanoribbon with $N=8$ atom pairs in the unit cell. At finite doping the energy gain due to the gap present in the AFb and AF solutions is reduced favoring the F solution which does not have a gap. *Lower row*. Up- and down-spin electron occupation per lattice site in the unit cell across the ribbon. The AFb configuration has broken charge-distribution symmetry relative to the ribbon center due to an unequal occupation of up- and down-spin bands. All mean-field bands are invariant under $k \rightarrow -k$. We show only the portion of the 1D BZ with states close to the Fermi level.

In the low doping regime a noncollinear spin order that continuously bridges the intermediate situation between the neutral AF configuration and mostly F configuration at higher doping is[26] a possibility. In the version of the Hubbard-model mean-field theory which allows for noncollinear spin densities we must allow for the possibility that the average spin polarization on different lattice sites points in different directions.[37] This allows a larger variational space within a single Slater-determinant approximation and can potentially lead to lower-energy solutions but the spin label becomes undefined for each single-particle wave function. We verified that noncollinear spin solutions are favored energetically[26] in the Hubbard-model calculations for low doping region and that the transition to F configuration happens at doping densities typically about 20% higher than when only collinear solutions are considered. The angle between the spin densities on opposite edges and the band structure of the noncollinear state are represented in Fig. 5.

In the intermediate doping regime the total energy is minimized by solutions which are more similar to the F neutral-ribbon configuration[19] which do not have an energy gap and are therefore favored by doping. This transition to F-type solutions occurs already at a relatively small value of doping $\delta n \simeq 0.06$. The states that are occupied first at finite doping are those near the valley points $|k|=2\pi/3a$ that are[19] spread across the ribbon and therefore control the exchange coupling between opposite edges. The W-scaling rules of the energy bands near the valley points[19] are consistent with the W^{-1} decay law of the threshold doping at which the transition to F-type transition occurs in our numerical phase diagram. In electronic structures with dominantly F character the charge-distribution symmetry around the ribbon center is preserved. In this case every occupied states, up- or down-spin and valence- or conduction-edge band, have a symmetric distribution of electron density around the ribbon center. When the doping is sufficiently large, however, we find a broken charge-symmetry solution that we label as Fb. In this state one of the occupied conduction bands has AF (unbalanced across the ribbon) rather than F (balanced across the ribbon) character. In addition to these solutions, we find that for wide ribbons there is an intermediate doping region in which AF solutions have lower total energy than the F solutions before the Fb solution is stabilized. The difference in energy between different magnetic solutions is small at intermediate and large doping.

In the high doping regime the magnetic features of the system progressively disappear as the edge-state bands become filled. The ribbon is found to turn paramagnetic above a critical value that increases with the ribbon width and saturates around $\delta n_c \sim 0.7$. Considering that edge-localized states in the conduction bands with k points near $2\pi/3a \leq |k| \leq \pi/a$ span approximately 1/3 of the whole Brillouin zone we find that the total amount of doping electrons required to fill completely the edge for both up and down spins is 2/3, an amount that can be surpassed near the mentioned doping saturation limit.

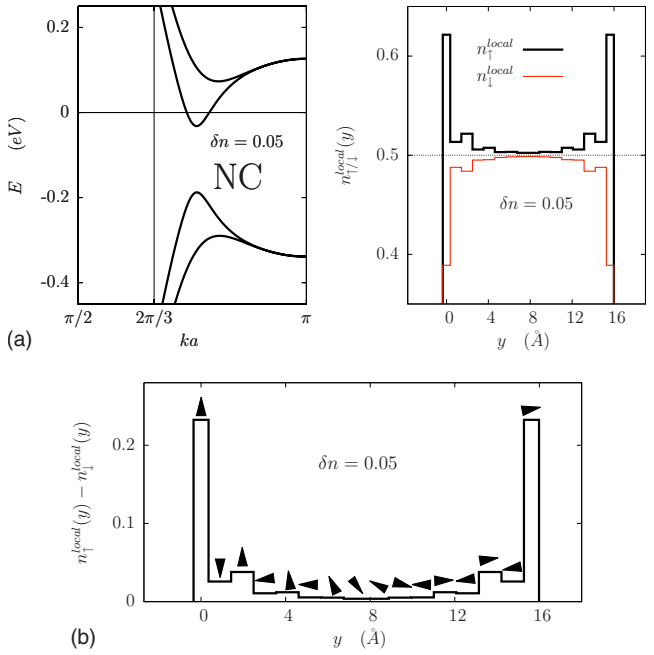

FIG. 5. (Color online) In the weakly doped region canted spin orientations develop in order to minimize the total energy when noncollinear solutions are allowed. *Upper row*. Band structure and spin-resolved electron occupation per lattice for a zigzag ribbon with $N=8$ and $\delta n=0.05$. The occupation and spin polarization at each lattice site are represented in a local frame where the spin is diagonal. *Lower row*. Spin polarization and relative orientation of the spin direction between different lattice sites represented with the arrow heads.

III. DISCUSSION

The AF state of zigzag nanoribbons has the unusual feature that inversion symmetry across the ribbon is broken in opposite senses in the two spin subsystems.[17,19] Our calculation suggests that in low doping regime the system can easily develop solutions with a charge density that is distributed asymmetrically across the ribbon, creating an interesting and unusually strong type of multiferroic behavior[17,38] in which spin polarization and charge density are coupled. We expect that transport properties can correspondingly be manipulated in interesting interrelated ways by both external magnetic fields and external electric fields directed across the ribbon. Edge transport should be strongly suppressed, for example, when a transverse electric field is applied which has opposite orientations on opposite ends of a ribbon.

Above a certain critical doping density, which is inversely proportional to the ribbon width W^{-1}, we find that the system undergoes a transition to a F configuration in which opposite edges have parallel spin polarizations. When doping is increased further the spin configuration is altered yet again, restoring inversion symmetry breaking across the ribbon. In this high doping regime the total magnetic condensation energy is small and the energy differences between different magnetic configurations are small. Eventually at sufficiently high doping the Hubbard-model SCF equations have only paramagnetic solutions.

The SiO_2 substrates on which exfoliated graphene samples are usually prepared have electron-density inhomogeneities[39] of the order of $n_{\rm fluc}\sim 10^{11}$ cm^{-2} that can extend over lengths of the order of $L\simeq 1$ μm. In the limiting case of ribbons with this same width as the puddle sizes a rough estimate of doping per unit lattice constant a within each puddle can be evaluated with the product of these two quantities

$$\delta n_{\rm fluc}\sim Ln_{\rm fluc}\sim 0.25/a.$$

This amount of doping can influence the spin configurations in the system and the presence of these random perturbations is therefore expected to appreciably weaken the tendency toward magnetic order, especially for wide ribbons. For this reason we should expect better chances of detecting edge magnetism in suspended ribbons which have much weaker electron-density fluctuations.

The long-ranged character of the Coulomb interaction, neglected in the present work, is expected to introduce important changes in the details of electronic structure especially in the regions in which states with different charge and spin configurations compete closely. The discrepancies can be more acute than in the neutral case because the inadequacy of short-ranged screening can be more relevant when the occupation of each lattice site in the unit cell becomes inhomogeneous as we depart from half filling. Nevertheless, it is also likely that several qualitative features of the solutions are still correctly captured by the Hubbard model and therefore can provide useful hints on the actual behavior of the magnetic configurations in ribbons as a function of doping. Even though fluctuation effects we have neglected may work against the formation of long-range order in these 1D magnets, the unusually stiff ferromagnetic alignment of the spins predicted by mean-field theories for zigzag ribbons[16] suggests that magnetic order could be possible and should be manifested in some way in experiments.

ACKNOWLEDGMENTS

We gratefully acknowledge helpful discussions with P. M. Haney, T. Pereg-Barnea, K. T. Delaney, and P. Rinke. Financial support was received from the Welch Foundation, NRI-SWAN, ARO, DOE, and the Spanish Ministry of Education through the MEC-Fulbright program.

*jeil@physics.utexas.edu

[1] K. S. Novoselov, A. K. Geim, S. V. Morozov, D. Jiang, M. I. Katsnelson, I. V. Grigorieva, S. V. Dubonos, and A. A. Firsov, Nature (London) **438**, 197 (2005).

[2] Y. Zhang, Yan-Wen Tan, Horst L. Stormer, and Philip Kim, Nature (London) **438**, 201 (2005).

[3] A. H. Castro Neto, F. Guinea, N. M. R. Peres, K. S. Novoselov, and A. K. Geim, Rev. Mod. Phys. **81**, 109 (2009); A. K. Geim and K. S. Novoselov, Nature Mater. **6**, 183 (2007); A. K. Geim and A. H. MacDonald, Phys. Today **60** (8), 35 (2007).

[4] M. Fujita, K. Wakabayashi, K. Nakada, and K. Kusakabe, J. Phys. Soc. Jpn. **65**, 1920 (1996).
[5] K. Nakada, M. Fujita, G. Dresselhaus, and M. S. Dresselhaus, Phys. Rev. B **54**, 17954 (1996).
[6] K. Wakabayashi, M. Fujita, H. Ajiki, and M. Sigrist, Phys. Rev. B **59**, 8271 (1999).
[7] T. Hikihara, X. Hu, H.-H. Lin, and C.-Y. Mou, Phys. Rev. B **68**, 035432 (2003).
[8] S. Dutta, S. Lakshmi, and S. K. Pati, Phys. Rev. B **77**, 073412 (2008).
[9] H. Lee, Y.-W. Son, N. Park, S. Han, and J. Yu, Phys. Rev. B **72**, 174431 (2005).
[10] M. Ezawa, Phys. Rev. B **73**, 045432 (2006).
[11] L. Brey and H. A. Fertig, Phys. Rev. B **73**, 235411 (2006).
[12] K.-I. Sasaki, S. Murakami, and R. Saito, J. Phys. Soc. Jpn. **75**, 074713 (2006).
[13] Y.-W. Son, M. L. Cohen, and Steven G. Louie, Phys. Rev. Lett. **97**, 216803 (2006).
[14] Y.-W. Son and Marvin L. Cohen, and Steven G. Louie, Nature (London) **444**, 347 (2006).
[15] L. Pisani, J. A. Chan, B. Montanari, and N. M. Harrison, Phys. Rev. B **75**, 064418 (2007).
[16] O. V. Yazyev and M. I. Katsnelson, Phys. Rev. Lett. **100**, 047209 (2008).
[17] J. Fernández-Rossier, Phys. Rev. B **77**, 075430 (2008).
[18] W. Y. Kim and K. S. Kim, Nat. Nanotechnol. **3**, 408 (2008).
[19] J. Jung, T. Pereg-Barnea, and A. H. MacDonald, Phys. Rev. Lett. **102**, 227205 (2009).
[20] M. Y. Han, Barbaros Özyilmaz, Y. Zhang, and P. Kim, Phys. Rev. Lett. **98**, 206805 (2007).
[21] X. Li, X. Wang, L. Zhang, S. Lee, and H. Dai, Science **319**, 1229 (2008).
[22] S. S. Datta, D. R. Strachan, S. M. Khamis and A. T. C. Johnson, Nano Lett. **8** 1912 (2008).
[23] M. Zarea and N. Sandler, Phys. Rev. Lett. **99**, 256804 (2007).
[24] M. Zarea, C. Busser, and N. Sandler, Phys. Rev. Lett. **101**, 196804 (2008).
[25] B. Huang, Q. Yan, G. Zhou, J. Wu, F. Liu, B.-L. Gu, and W. Duan, Appl. Phys. Lett. **91**, 253122 (2007); F. Cervantes-Sodi, G. Csanyi, S. Piscanec, and A. C. Ferrari, Phys. Rev. B **77**, 165427 (2008); N. Gorjizadeh, A. A. Farajian, K. Esfarjani, and Y. Kawazoe, *ibid.* **78**, 155427 (2008); S. S. Yu, W. T. Zheng, Q. B. Wen, and Q. Jiang, Carbon **46**, 537 (2008); T. Wassmann, A. P. Seitsonen, A. M. Saitta, M. Lazzeri, and F. Mauri, Phys. Rev. Lett. **101**, 096402 (2008); S. Dutta and S. K. Pati, J. Phys. Chem. B **112**, 1333 (2008); S. Dutta, A. K. Manna, and S. K. Pati, Phys. Rev. Lett. **102**, 096601 (2009).
[26] K. Sawada, F. Ishii, M. Saito, S. Okada, and T. Kawai, Nano Lett. **9**, 269 (2009).
[27] J. M. Kinder, J. J. Dorando, H. Wang, and G. K.-L. Chan, Nano Lett. **9**, 1980 (2009).
[28] A. Cresti, G. Grosso, and G. P. Parravicini, Phys. Rev. B **77**, 233402 (2008).
[29] A. Cresti, G. Grosso, and G. P. Parravicini, Phys. Rev. B **78**, 115433 (2008).
[30] J. Nakabayashi, D. Yamamoto, and S. Kurihara, Phys. Rev. Lett. **102**, 066803 (2009).
[31] A. Rycerz, J. Tworzydlo, and C. W. J. Beenakker, Nat. Phys. **3**, 172 (2007).
[32] A. R. Akhmerov, J. H. Bardarson, A. Rycerz, and C. W. J. Beenakker, Phys. Rev. B **77**, 205416 (2008).
[33] K. Wakabayashi and T. Aoki, Int. J. Mod. Phys. B **16**, 4897 (2002).
[34] O. V. Yazyev, Phys. Rev. Lett. **101**, 037203 (2008).
[35] J. Fernández-Rossier and J. J. Palacios, Phys. Rev. Lett. **99**, 177204 (2007).
[36] J. J. Palacios, J. Fernández-Rossier, and L. Brey, Phys. Rev. B **77**, 195428 (2008).
[37] P. Haney, Doctoral thesis, Department of Physics, University of Texas at Austin, 2007.
[38] J. van den Brink and Daniel I Khomskii, J. Phys.: Condens. Matter **20**, 434217 (2008); N. A. Spaldin and M. Fiebig, Science **309**, 391 (2005).
[39] J. Martin, N. Akerman, G. Ulbricht, T. Lohmann, J. H. Smet, K. von Klitzing, and A. Yacobi, Nat. Phys. **4**, 144 (2008).